

# Molecular structure–property engineering for photovoltaic applications: Fluorene-acceptor alternating conjugated copolymers with varied bridged moieties

Yaowen Li, Hui Li, Bin Xu, Zaifang Li, Feipeng Chen, Dongqing Feng, Jibo Zhang, Wenjing Tian\*

State Key Laboratory of Supramolecular Structure and Materials, Jilin University, Changchun 130012, PR China

## ARTICLE INFO

### Article history:

Received 22 August 2009

Received in revised form

4 January 2010

Accepted 16 January 2010

Available online 28 January 2010

### Keywords:

Photovoltaic cells

Conjugated polymers

Synthesis

## ABSTRACT

A series of novel soluble conjugated copolymers consisting of electron-accepting 2-pyran-4-ylidene-malononitrile (PM) and electron-donating fluorene connected by different electron-donating ability conjugated moieties were synthesized by Suzuki coupling polymerization. The structures of the copolymers were characterized and their physical properties were investigated. High molecular weight ( $M_n$  up to 43.8 kg/mol) and thermostable copolymers were obtained. The conjugated bridge between PM and fluorene building block with gradually increased electron-donating ability moieties results in enhanced intramolecular charge transfer (ICT) transition bands, which lead to an extension of their absorption spectral range. Cyclic voltammetry measurement displayed that the highest occupied molecular orbital (HOMO) and lowest unoccupied molecular orbital (LUMO) energy levels of the copolymers can be fine-tuned. The resulting copolymers possessed relatively low HOMO energy levels, promising good air stability and high open circuit voltage ( $V_{oc}$ ) for photovoltaic application. Bulk heterojunction photovoltaic devices were fabricated by using the copolymers as donors and (6,6)-phenyl  $C_{61}$ -butyric acid methyl ester (PCBM) as acceptor. The power conversion efficiencies (PCE) of the devices were in the range of 0.02–0.52% under simulated AM 1.5 solar irradiation of 100 mW/cm<sup>2</sup>, and the highest  $V_{oc}$  reached 0.82 V. The significant improvement of PCE indicates a novel concept for developing donor–acceptor (D–A) conjugated copolymers with high photovoltaic performance by adjusting electron-donating ability of conjugated bridge.

© 2010 Elsevier Ltd. All rights reserved.

## 1. Introduction

In recent years, considerable efforts have been directed towards the development of new polymer photovoltaic cells (PVCs). PVCs are becoming more and more attractive because they represent a low cost and flexible devices, tunable electronic properties, and ease of processing [1–4]. One of the promising strategies for devising efficient PVCs involves the use of interpenetrating networks bulk heterojunctions (BHJ) based on a blend of electron-donating conjugated polymers and soluble fullerene acceptors as the active layer [5]. For instance, bulk heterojunction PVCs made from a blend of regioregular poly(3-hexylthiophene) (P3HT) as the donor and PCBM as the acceptor have recently been shown the power conversion efficiencies (PCE) up to 4–5% [6,34]. However, P3HT only harvests photons with wavelengths below 650 nm, while the energy of the majority of the solar photons is much lower

(around 700 nm) [7]. In order to further improve the properties of PVCs, people paid more attention to the donor–acceptor (D–A) conjugated polymers whose optical and electronic properties could be tunable through the intramolecular charge transfer (ICT) from the donor to acceptor. So, design and synthesis D–A conjugated copolymers which can efficiently harvest the majority energy of the solar spectrum, are effective ways to obtain low band gap polymers [8]. However, several reported D–A copolymers showed PCE much lower than the wide band gap counterparts [9], because of the mismatch of the energy level between electron-donating polymer and electron acceptor (e.g., PCBM), and large-scale blend phase separation between the donor and acceptor [10]. Most recently, several D–A copolymer systems have achieved better efficiency by tuning the energy level of the polymers through modifying the monomer structures based on the known thienopyrazine or benzothiadiazole systems [11,15]. However, the relatively low  $V_{oc}$  (around 0.6 V) still limits the PCE of the devices.

On all accounts, the D–A copolymers with low band gaps are needed for harvesting solar photons in a broader spectrum. To fulfill this requirement, well-chosen donor and acceptor groups are

\* Corresponding author. Tel.: +86 431 85155359; fax: +86 431 85193421.  
E-mail address: [wjtian@jlu.edu.cn](mailto:wjtian@jlu.edu.cn) (W. Tian).

particularly desirable for low band gap polymers due to a significant enhancement of the ICT intensity and conjugated length, which lead to a better extended absorption and higher absorption coefficient. In addition, the D–A copolymers should possess the following two features in order to achieve high efficiency of PVCs. One is sufficient driving force for electron transfer from the electron donor to the acceptor, and suitable HOMO energy level of electron donor. It means that the LUMO energy level of the electron donor must be higher than that of the electron acceptor (at least 0.3 eV) in order to have sufficient driving force for electron transfer from the donor to acceptor, and the HOMO energy level of electron donor must be low enough in order to get relative high  $V_{oc}$ , which is determined by the difference between the HOMO energy level of the donor and LUMO energy level of the acceptor [13]. The other is to have good miscibility with the electron acceptor (e.g., PCBM) to form an interpenetrating network. In order to efficiently dissociate the excitons occurred at the interface between the electron-donating component and the electron-accepting one, the control of the BHJ morphology is of crucial importance. Ideally, the phase separation length scale should match the exciton diffusion length of conjugated polymer, which is approximately 10 nm [12]. Consequently, to further increase the photovoltaic performances for practical application, it is important to design and synthesize polymers with the possibility to tune their energy levels and miscibility with the electron acceptor (e.g., PCBM).

It is widely accepted that the alternative copolymer structures with donor and acceptor functionalities are very effective in decreasing the band gap and modulating electronic and physical properties of the polymers. Most of the D–A copolymer system was symbolized as  $[D^*–D–A–D]_n$ , where the  $D^*$  is the donor, A is acceptor unit and D is an aromatic donor conjugated bridge between the  $D^*$  and A which can increase the conjugated length of copolymers. Numerous attempts to develop new donor/acceptor  $[D^*–D–A–D]_n$  combinations have been made by changing electron-donating  $D^*$ . For example, the 4,7-dithien-2-yl-2,1,3-benzothiadiazole (DTBT) unit is very effective as an acceptor, and it can copolymerize with many kinds of donor segments ( $D^*$ ), such as fluorene [13], silafluorene [14], carbazole [15], dithienosilole [16], and cyclopenta[2,1-*b*:3,4-*b'*]dithiophene [17]. Meanwhile, many electron-accepting moieties (A), including quinoline [18], quinoxaline [19], 2,1,3-benzothiadiazole [13], and pyridazine [20] have been also introduced into  $[D^*–D–A–D]_n$  copolymer systems. All the above research efforts have led to major progress in the synthesis of new D–A copolymers. However, the conjugated bridged-D which connects the  $D^*$  and A also plays an important role in tuning the optical and electronic properties by changing varied electron-donating ability and coplanarity. To our knowledge, the research of the conjugated bridged-D copolymers for photovoltaic devices has been scarcely considered.

Herein, we synthesized three novel  $\pi$ -conjugated copolymers consisting of PM-based donor unit coupled to different electron-donating moieties: poly{(9,9-dihexyl-9H-fluorene-2,7-ylene)-alt-2-(2,6-bis((E)-2,5-bis(hexyloxy)styryl)-4H-pyran-4-ylidene)malononitrile}(PFBMB), poly{(9,9-dihexyl-9H-fluorene-2,7-ylene)-alt-2-(2,6-bis((E)-2-(5-bromo-3,4-dihexylthiophen-2-yl)vinyl)-4H-pyran-4-ylidene)-malononitrile} (PFTMT), poly{(2,2'-bithiophene-5,5'-ylene)-alt-2-(2,6-bis((E)-2-(10-hexyl-10H-phenothiazin-3-yl)vinyl)-4H-pyran-4-ylidene)malononitrile}(PFPM). The functional electron-donating moieties fluorene ( $D^*$ ) can increase the solubility and coplanarity of the copolymers. 2-Pyran-4-ylidenemalononitrile (A) is a strong electron-accepting group, which can increase electron affinity and reduce the band gap of the conjugated system [21]. To allow for the systematic modulation of the electronic and optical properties, derivatives with a chain structure  $[D^*–D–A–D]_n$  were designed, where the varied alkylated bridged-D assured the better

conjugated length, which could further reduce the band gap of the conjugated system. We reasoned that incorporation of varied electron-donating ability functional bridged-D moieties will bring different degrees of ICT to the conjugated system and thus provide a means to tune the energy levels. Indeed, we found that the energy level and absorption spectra of copolymers can be fine-tuned by changing the moieties of different electron-donating ability. Both the HOMO energy level (–5.13 to –5.64 eV) and LUMO energy level (around –3.35 eV) of the copolymers were close to the ideal energy level [39]. The photovoltaic performances of copolymers demonstrated that appropriate energy level and molecular structure engineering resulted in the improvement of the PCE to 0.52% (in the case of PFPM), which was more than 13 times higher than that of PFTMT.

## 2. Experimental section

### 2.1. Materials

2,7-Bis(4,4,5,5-tetramethyl-1,3,2-dioxaborolan-2-yl)-9,9-dihexylfluorene [22], 1,4-dihexyl-2,5-dibromobenzene (1) [23], 2,5-dibromo-3,4-dihexylthiophene (3) [22], 3,7-dibromo-10-hexylphenothiazine (5) [24], 2-(2,6-dimethyl pyran-4-ylidene)malononitrile [25], was synthesized according to known literature procedures. All reagents and chemicals were purchased from commercial sources (Aldrich, Across, Fluka) and used without further purification unless stated otherwise. All solvents were distilled over appropriate drying agent(s) prior to use and were purged with nitrogen.

### 2.2. Characterization

The infrared spectroscopy spectra were recorded via the KBr pellet method by using a Nicolet Impact 410 FT-IR spectrophotometer. The elemental analysis was carried out with a Thermoquest CHNS-Ovelemental analyzer. The gel permeation chromatographic (GPC) analysis was carried out with a Waters 410 instrument with tetrahydrofuran as the eluent (flow rate: 1 mL/min, at 35 °C) and polystyrene as the standard. Differential scanning calorimetry (DSC) were performed under nitrogen flushing at a heating rate of 20 °C/min with a NETZSCH (DSC-204) instrument. Thermogravimetric analysis were performed on a Perkin Elmer Pyris 1 analyzer under nitrogen atmosphere (100 mL/min) at a heating rate of 10 °C/min.  $^1\text{H}$  NMR and  $^{13}\text{C}$  NMR spectra were measured using a Bruker AVANCE-500 NMR spectrometer and a Varian Mercury-300 NMR, respectively. UV–visible absorption spectra were measured using a Shimadzu UV-3100 spectrophotometer. The photoluminescence spectra of spin-cast films and solution were measured with an RF-5301PC spectrofluorophotometer. Electrochemical measurements of these derivatives were performed with a Bioanalytical Systems BAS 100 B/W electrochemical workstation. Atomic force microscopy (AFM) images of blend films were carried out using a Nanoscope IIIa Dimension 3100.

### 2.3. Photovoltaic device fabrication and characterization

For device fabrication, the ITO glass was precleaned and modified by a thin layer of PEDOT:PSS, which was spin-cast from a PEDOT:PSS aqueous solution (H. C. Starck) on the ITO substrate, and the thickness of the PEDOT:PSS layer is about 50 nm. The active layer contained a blend of copolymers as electron donor and PCBM as electron acceptor, which was prepared by weight ratio (1:1 w/w, 1:2 w/w, 1:3 w/w, 1:4 w/w) in chlorobenzene (8 mg/mL) for copolymers. After spin-coating the blend from solution at 3000 rpm, The devices were completed by evaporating a 0.6 nm LiF

layer protected by 100 nm of Al at a base pressure of  $5 \times 10^{-4}$  Pa. The effective photovoltaic area as defined by the geometrical overlap between the bottom ITO electrode and the top cathode was 4 or 5 mm<sup>2</sup>. The thickness of the photoactive layer was 50–60 nm, measured by the Ambios Technology XP-2. The current–voltage (*I*–*V*) characterization of PV devices in the dark and under white-light illumination from an SCIENCETECH 500-W solar simulator (AM 1.5100 mW/cm<sup>2</sup>) were measured on computer-controlled Keithley 2400 Source Meter measurement system. All the measurements were performed under ambient atmosphere at room temperature.

## 2.4. Synthesis of monomers

### 2.4.1. Synthesis of 4-bromo-2,5-di(hexyloxy)benzaldehyde (2)

*n*-BuLi (1.07 mL of 2.5 M solution in hexane, 2.68 mmol) was added dropwise to a solution of compound **1** (1.064 g, 2.44 mmol) in THF (30 mL) at  $-78$  °C under argon. The solution was stirred at  $-78$  °C for 2 h, then dried DMF (0.24 mL) was added quickly and it was kept at room temperature and stirred for 24 h before being poured into water. The product was extracted with ether. The organic layer was subsequently washed with water and brine and dried over MgSO<sub>4</sub>, and the solvent was removed by rotary evaporation. The crude product was purified by column chromatography with CH<sub>2</sub>Cl<sub>2</sub>:petroleum ether (1:2) to give a red bright yellow solid (0.71 g, 1.85 mmol, yield 76%). <sup>1</sup>H NMR (500 MHz, CDCl<sub>3</sub>, TMS):  $\delta$ (ppm) 10.41 (s, 1H, –CHO), 7.31 (s, 1H, –Ph), 7.23 (s, 1H, –Ph), 4.01 (m, 4H, –OCH<sub>2</sub>), 1.82 (m, 4H, –CH<sub>2</sub>), 1.47 (m, 4H, –CH<sub>2</sub>), 1.35 (m, 8H, –CH<sub>2</sub>), 0.91 (m, 6H, –CH<sub>3</sub>). <sup>13</sup>C NMR (125 MHz, CDCl<sub>3</sub>, TMS):  $\delta$ (ppm) 189.29, 156.17, 150.29, 124.71, 121.36, 118.88, 111.05, 70.25, 69.89, 31.87, 29.44, 29.40, 26.07, 26.02, 22.96, 14.40. Elem. Anal. Calcd. for C<sub>19</sub>H<sub>29</sub>BrO<sub>3</sub>: C, 59.22; H, 7.59. Found: C, 59.15; H, 7.60.

### 2.4.2. Synthesis of 5-bromo-3,4-dihexylthiophene-2-carbaldehyde (4)

The synthetic procedure for **3** was similar to that for **2** give a red brown oil (0.46 g, 1.29 mmol, yield 53%). <sup>1</sup>H NMR (500 MHz, CDCl<sub>3</sub>, TMS):  $\delta$ (ppm) 9.91 (s, 1H, –CHO), 2.87 (t, *J* = 8.0 Hz, 2H,  $-\alpha$ CH<sub>2</sub>), 2.54 (t, *J* = 8.0 Hz, 2H,  $-\alpha$ CH<sub>2</sub>), 1.57 (m, 2H, –CH<sub>2</sub>), 1.50 (m, 2H, –CH<sub>2</sub>), 1.50 (m, 4H, –CH<sub>2</sub>), 1.32 (m, 8H, –CH<sub>2</sub>), 0.90 (m, 6H, –CH<sub>3</sub>). <sup>13</sup>C NMR (75 MHz, CDCl<sub>3</sub>, TMS):  $\delta$ (ppm) 181.23, 151.350, 143.70, 138.25, 122.48, 32.23, 31.459, 31.43, 29.36, 29.21, 27.91, 27.71, 22.53, 22.48, 13.99. Elem. Anal. Calcd. for C<sub>17</sub>H<sub>27</sub>BrOS: C, 56.82; H, 7.57. Found: C, 56.80; H, 7.60.

### 2.4.3. Synthesis of 7-bromo-10-hexyl-10H-phenothiazine-3-carbaldehyde (6)

The synthetic procedure for **6** was similar to that for **2** give a yellow solid (0.62 g, 1.58 mmol, yield 65%). <sup>1</sup>H NMR (500 MHz, CDCl<sub>3</sub>, TMS):  $\delta$ (ppm) 9.79 (s, 1H, –CHO), 7.64–7.63 (m, 1H, –Ph), 7.55 (m, 1H, –Ph), 7.25–7.20 (m, 2H, –Ph), 6.88 (d, *J* = 8.5 Hz, 1H, –Ph), 6.70 (d, *J* = 9.0 Hz, 1H, –Ph), 3.83 (t, *J* = 7.3 Hz, 2H, –NCH<sub>2</sub>), 1.77 (m, 2H, –CH<sub>2</sub>), 1.42 (m, 2H, –CH<sub>2</sub>), 1.30 (m, 4H, –CH<sub>2</sub>), 0.87 (m, *J* = 6.3 Hz, 3H, –CH<sub>2</sub>). <sup>13</sup>C NMR (75 MHz, DMSO, TMS):  $\delta$ (ppm) 189.79, 150.22, 142.57, 131.22, 130.18, 130.17, 129.70, 128.34, 126.06, 124.30, 117.01, 115.72, 114.92, 48.03, 31.28, 26.55, 26.38, 22.49, 13.91. Elem. Anal. Calcd. for C<sub>19</sub>H<sub>20</sub>BrNOS: C, 58.46; H, 5.16; N, 3.59. Found: C, 58.50; H, 5.15; N, 3.55.

### 2.4.4. Synthesis of 2-(2,6-bis((E)-4-bromo-2,5-bis(hexyloxy)styryl)-4H-pyran-4-ylidene)malononitrile (M-1)

A mixture of 4-bromo-2,5-di(hexyloxy)benzaldehyde (**2**) (4.44 g, 10.17 mmol), 2-(2,6-dimethylpyran-4-ylidene)malononitrile (**7**) (0.80 g, 4.62 mmol), piperidine (20 drops), and *n*-propyl alcohol were refluxed under N<sub>2</sub> for 24 h. The reaction mixture was cooled to room temperature and poured into water and extracted

with chloroform. The combined organic extractions were washed three times with water, dried over anhydrous MgSO<sub>4</sub>, evaporated under vacuum and purified with column chromatography on silica gel with dichloromethane:petroleum ether (3:1) as the eluant to a dark red solid (2.64 g, 2.91 mmol, yield 63.0%). <sup>1</sup>H NMR (500 MHz, CDCl<sub>3</sub>, TMS):  $\delta$ (ppm) 7.76 (d, *J* = 16.5 Hz, 2H, –vinylic), 7.15 (s, 2H, –Ph), 7.02 (s, 2H, –Ph), 6.87 (d, *J* = 16.0 Hz, 2H, –vinylic), 6.68 (s, 2H, –Ph), 4.01 (m, 8H, –OCH<sub>2</sub>), 1.84 (m, 8H, –CH<sub>2</sub>), 1.53–1.44 (m, 8H, –CH<sub>2</sub>), 1.37 (m, 8H, –CH<sub>2</sub>), 1.23 (m, 8H, –CH<sub>2</sub>), 0.92 (m, 6H, –CH<sub>3</sub>), 0.79 (m, 6H, –CH<sub>3</sub>). <sup>13</sup>C NMR (75 MHz, DMSO, TMS):  $\delta$ (ppm) 158.46, 155.61, 151.44, 149.19, 131.03, 123.77, 119.72, 117.93, 114.95, 114.34, 111.94, 106.77, 69.39, 30.71, 30.56, 28.37, 25.06, 24.81, 21.68, 21.56, 13.44, 13.29. Elem. Anal. Calcd. for C<sub>48</sub>H<sub>62</sub>Br<sub>2</sub>N<sub>2</sub>O<sub>5</sub>: C, 63.58; H, 6.89; N, 3.09. Found: C, 63.60; H, 6.85; N, 3.05.

### 2.4.5. Synthesis of 2-(2,6-bis((E)-2-(5-bromo-3,4-dihexylthiophen-2-yl)vinylyl)-4H-pyran-4-ylidene)malononitrile (M-2)[22]

The synthetic procedure for **M-2** was similar to that for **M-1** gave a dark green solid (2.1 g, 2.46 mmol, yield 53.2%). <sup>1</sup>H NMR (500 MHz, CDCl<sub>3</sub>, TMS):  $\delta$ (ppm) 7.51 (d, *J* = 15.5 Hz, 2H, –vinylic), 6.61 (s, 2H, –PM), 6.37 (d, *J* = 15.5 Hz, 2H, –vinylic), 2.68 (t, *J* = 7.8 Hz, 4H,  $-\alpha$ CH<sub>2</sub>), 2.53 (t, *J* = 7.8 Hz, 4H,  $-\alpha$ CH<sub>2</sub>), 1.50 (m, 8H, –CH<sub>2</sub>), 1.33 (m, 16H, –CH<sub>2</sub>), 1.29 (m, 8H, –CH<sub>2</sub>), 0.91 (t, *J* = 6.8 Hz, 6H, –CH<sub>3</sub>), 0.84 (t, *J* = 6.8 Hz, 6H, –CH<sub>3</sub>). <sup>13</sup>C NMR (75 MHz, CDCl<sub>3</sub>, TMS):  $\delta$ (ppm) 157.79, 157.69, 155.16, 144.95, 143.32, 134.63, 127.84, 116.50, 115.13, 113.72, 106.64, 59.60, 31.45, 31.42, 29.34, 29.19, 28.31, 27.96, 22.49, 13.95, 13.87. Elem. Anal. Calcd. for C<sub>44</sub>H<sub>58</sub>Br<sub>2</sub>N<sub>2</sub>O<sub>5</sub>: C, 61.82; H, 6.84; N, 3.28. Found: C, 61.88; H, 6.87; N, 3.22.

### 2.4.6. Synthesis of 2-(2,6-bis((E)-2-(7-bromo-10-hexyl-10H-phenothiazin-3-yl)vinylyl)-4H-pyran-4-ylidene)malononitrile (M-3)

The synthetic procedure for **M-3** was similar to that for **M-1** give a dark solid (6.84 g, 7.47 mmol, yield 73.5%). <sup>1</sup>H NMR (500 MHz, CDCl<sub>3</sub>, TMS):  $\delta$ (ppm) 7.37–7.34 (m, 4H, –Ph and –vinylic), 7.30 (m, 2H, –Ph), 7.27–7.24 (m, 4H, –Ph), 6.86 (d, *J* = 8.5 Hz, 4H, –Ph), 6.72 (d, *J* = 8.5 Hz, 2H, –Ph), 6.62 (s, 2H, –PM), 6.59 (d, *J* = 16.0 Hz, 2H, –vinylic), 3.84 (t, *J* = 7.0 Hz, 4H, –NCH<sub>2</sub>), 1.80 (m, 4H, –CH<sub>2</sub>), 1.44 (m, 4H, –CH<sub>2</sub>), 1.32 (m, 8H, –CH<sub>2</sub>), 0.89 (t, *J* = 7.0 Hz, 6H, –CH<sub>3</sub>). <sup>13</sup>C NMR (75 MHz, CDCl<sub>3</sub>, TMS):  $\delta$ (ppm) 158.22, 155.59, 146.73, 143.13, 136.35, 130.20, 129.68, 129.10, 127.72, 126.40, 125.96, 124.57, 116.84, 116.50, 115.50, 115.42, 115.20, 106.70, 59.03, 47.90, 31.38, 26.66, 26.50, 22.57, 13.98. Elem. Anal. Calcd. for C<sub>48</sub>H<sub>44</sub>Br<sub>2</sub>N<sub>4</sub>O<sub>5</sub>: C, 62.88; H, 4.84; N, 6.11. Found: C, 62.95; H, 4.82; N, 6.13.

## 2.5. General procedures of polymerization

Suzuki cross-coupling reaction was used to synthesize the copolymers shown in Scheme 2. 2,7-Bis(4,4,5,5-tetramethyl-1,3,2-dioxaborolan-2-yl)-9,9-dihexyl-fluorene, dibromo monomer, and (PPh<sub>3</sub>)<sub>4</sub>Pd(0) (2 mol% with respect to the monomer) were dissolved in a mixture of toluene (15 mL) and aqueous 2 M K<sub>2</sub>CO<sub>3</sub> (3/2 volume ratio). The solution was stirred under an Ar atmosphere and refluxed with vigorous stirring for 48 h. The resulting solution was then poured into methanol and followed by washing with water. The precipitated solid was extracted with methanol and acetone for 24 h in a Soxhlet apparatus to remove the oligomers and catalyst residues, respectively. The soluble fraction was then collected via extraction with CHCl<sub>3</sub> for 24 h. The chloroform solution was then concentrated to afford the copolymers.

### 2.5.1. Poly{(9,9-dihexyl-9H-fluorene-2,7-ylene)-alt-2-(2,6-bis((E)-2,5-bis(hexyloxy)styryl)-4H-pyran-4-ylidene)malononitrile} (PFBMB)

The resulting copolymer PFBMB was obtained as a dark green shining powder with a yield of 74%. <sup>1</sup>H NMR (500 MHz, CDCl<sub>3</sub>, TMS):

$\delta$ (ppm) 7.94 (d,  $J = 16.5$  Hz, 2H, -vinylic), 7.78 (2 m, H, -Ph), 7.68 (br, 2H, -Ph), 7.53 (m, 2H, -Ph), 7.17 (br, 2H, -Ph), 7.05 (br, 2H, -Ph), 6.97 (d,  $J = 15.5$  Hz, 2H, -vinylic), 6.73 (s, 2H, -PM), 4.12 (br, 4H, -OCH<sub>2</sub>), 3.99 (br, 4H, -OCH<sub>2</sub>), 2.04 (br, 4H, - $\alpha$ CH<sub>2</sub>), 1.88 (br, 4H, -CH<sub>2</sub>), 1.75 (br, 4H, -CH<sub>2</sub>), 1.56–1.05 (m, 40H, -CH<sub>2</sub>), 0.88 (br, 6H, -CH<sub>3</sub>) 0.81 (br, 6H, -CH<sub>3</sub>), 0.76 (br, 6H, -CH<sub>3</sub>). <sup>13</sup>C NMR (125 MHz, CDCl<sub>3</sub>, TMS):  $\delta$ (ppm) 159.45, 156.53, 152.99, 151.05, 150.80, 144.19, 140.67, 137.10, 135.46, 128.47, 124.75, 123.72, 119.89, 119.30, 116.02, 113.31, 107.71, 70.20, 55.57, 40.93, 32.56, 31.98, 31.40, 30.36, 29.77, 29.06, 28.82, 26.36, 26.18, 24.41, 23.06, 14.43. Elem. Anal. Calcd. for C<sub>73</sub>H<sub>94</sub>N<sub>2</sub>O<sub>5</sub>: C, 81.14; H, 8.71; N, 2.59. Found: C, 80.34; H, 8.63; N, 2.13.

### 2.5.2. Poly{(9,9-dihexyl-9H-fluorene-2,7-ylene)-alt-2-(2,6-bis((E)-2-(3,4-dihexylthiophen-2-yl) vinyl)-4H-pyran-4-ylidene)malononitrile} (PFTMT)[22]

The resulting copolymer PFTMT was obtained as a dark green shining powder with a yield of 80%. <sup>1</sup>H NMR (500 MHz, CDCl<sub>3</sub>, TMS):  $\delta$ (ppm) 7.80 (br, 2H, -Ph), 7.71 (d,  $J = 16.0$  Hz, 2H, -vinylic), 7.47 (br, 4H, -Ph), 6.64 (s, 2H, -PM), 6.55 (d, 2H,  $J = 16.0$  Hz, -vinylic), 2.79 (br, 4H, - $\alpha$ CH<sub>2</sub>), 2.67 (br, 4H, - $\alpha$ CH<sub>2</sub>), 2.04 (br, 4H, - $\alpha$ CH<sub>2</sub>), 1.10–1.65 (m, 48H, -CH<sub>2</sub>), 0.88 (br, 12H, -CH<sub>3</sub>), 0.81 (t,  $J = 7.3$  Hz, 12H, -CH<sub>3</sub>). <sup>13</sup>C NMR (125 MHz, CDCl<sub>3</sub>, TMS):  $\delta$ (ppm) 159.68, 155.90, 151.83, 147.35, 142.75, 141.03, 140.26, 133.85, 129.18, 129.01, 128.93, 128.69, 128.44, 123.83, 120.60, 120.40, 120.33, 116.48, 115.99, 107.08, 106.91, 59.13, 55.79, 40.90, 32.34, 32.23, 32.09, 32.02, 31.34, 30.50, 30.02, 29.96, 29.47, 28.32, 27.99, 25.37, 24.39, 23.10, 23.00, 14.45. Elem. Anal. Calcd. for C<sub>69</sub>H<sub>90</sub>N<sub>2</sub>O<sub>5</sub>: C, 80.65; H, 8.77; N, 2.72. Found: C, 79.66; H, 9.11; N, 2.44.

### 2.5.3. Poly{(2,2'-bithiophene-5,5'-ylene)-alt-2-(2,6-bis((E)-2-(10-hexyl-10H-phenothiazin-3-yl) vinyl)-4H-pyran-4-ylidene)malononitrile} (PFPMP)

The resulting copolymer PFPMP was obtained as a dark powder with a yield of 52%. <sup>1</sup>H NMR (500 MHz, CDCl<sub>3</sub>, TMS):  $\delta$ (ppm) 7.75 (br, 2H, -vinylic), 7.50 (br, 6H, -Ph), 7.43 (br, 2H, -Ph), 7.34 (br, 6H, -Ph), 6.95 (br, 2H, -Ph), 6.88 (br, 2H, -Ph), 6.58 (m, 4H, -vinylic and -PM), 3.91 (br, 4H, -NCH<sub>2</sub>), 2.03 (br, 4H, - $\alpha$ CH<sub>2</sub>), 1.86 (br, 4H, -CH<sub>2</sub>), 1.48 (br, 4H, -CH<sub>2</sub>), 1.35 (br, 8H, -CH<sub>2</sub>), 1.15 (br, 4H, -CH<sub>2</sub>), 1.06 (br, 12H, -CH<sub>2</sub>), 0.90 (br, 6H, -CH<sub>3</sub>), 0.77 (br, 6H, -CH<sub>3</sub>). <sup>13</sup>C NMR (125 MHz, CDCl<sub>3</sub>, TMS):  $\delta$ (ppm) 158.78, 156.12, 152.17, 147.38, 143.30, 140.39, 138.92, 137.13, 129.25, 128.07, 127.59, 126.60, 126.24, 125.80, 125.22, 124.40, 121.21, 120.48, 116.63, 116.24, 115.93, 115.69, 107.04, 55.72, 48.33, 40.86, 32.19, 31.87, 30.41, 29.34, 27.21, 27.02, 25.36, 24.26,

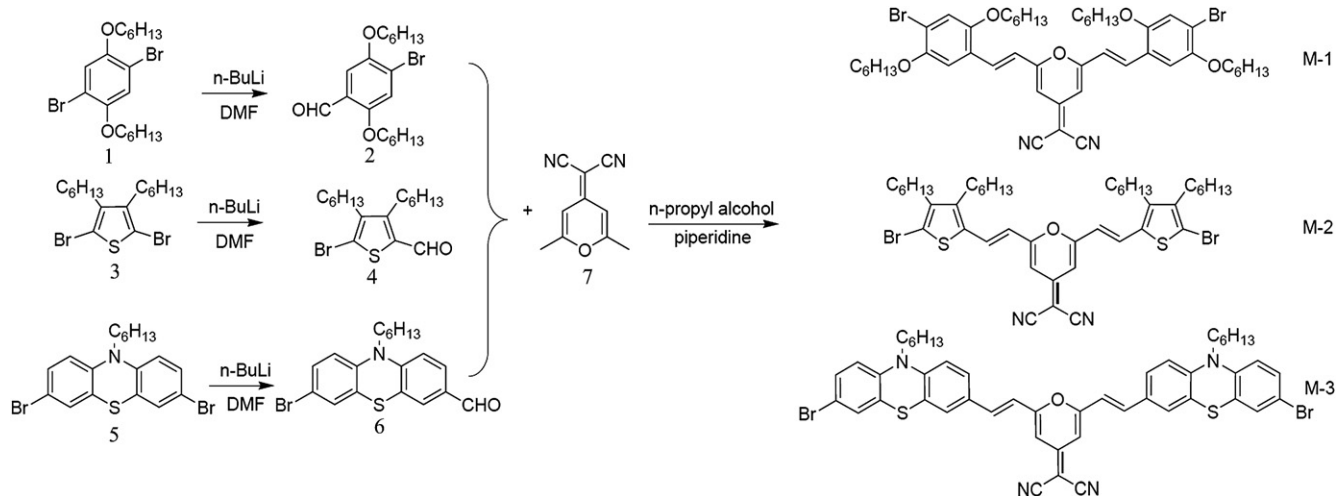
23.02, 22.98, 14.46. Elem. Anal. Calcd. for C<sub>73</sub>H<sub>76</sub>N<sub>4</sub>O<sub>5</sub>: C, 80.40; H, 6.98; N, 4.41. Found: C, 79.83; H, 7.68; N, 4.56.

## 3. Results and discussion

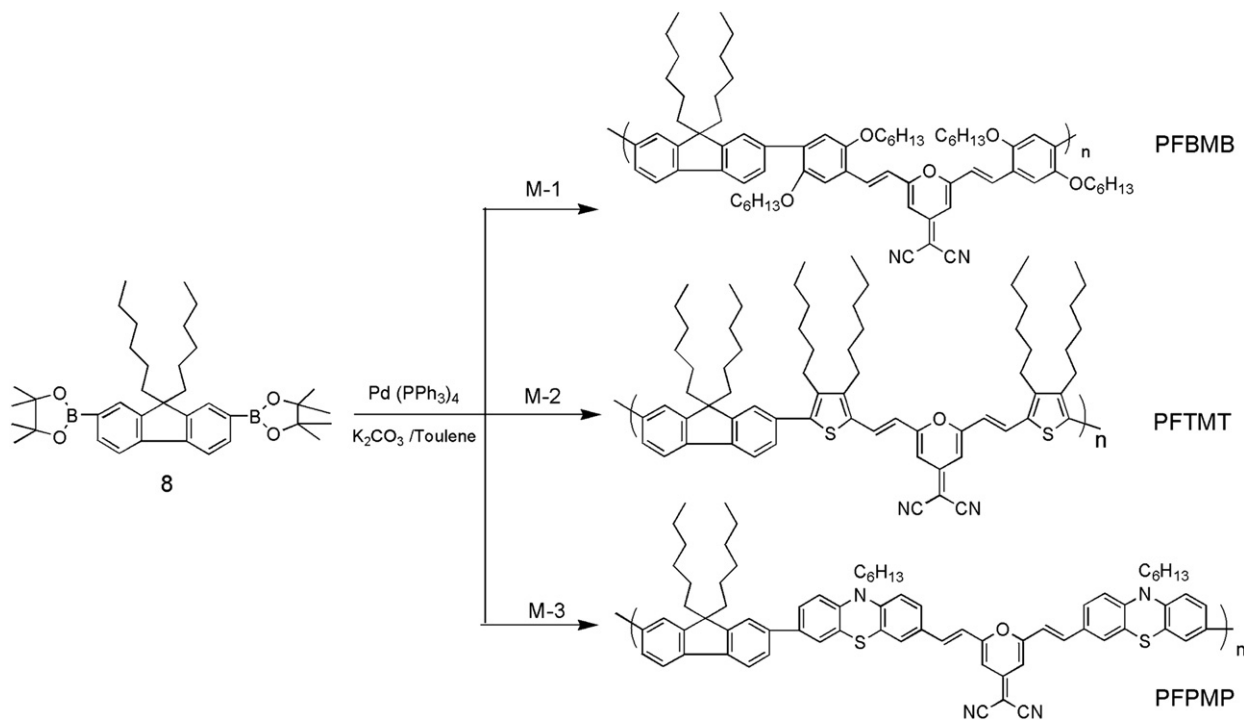
### 3.1. Material synthesis and structural characterization

The general synthetic routes toward the monomers are outlined in Scheme 1. In order to increase the solubility of the monomer, the active proton of the hydroquinone, thiophene and phenothiazine was alkylated with 1-bromohexane before dibromination. Critical to the synthetic strategy was the selective halogen-metal exchange followed by conversion to the aldehyde. The monoaldehyde of dibromo compounds (**1**, **3**, **5**) was prepared by a modified procedure with 1.1 equiv n-BuLi followed by DMF. The monomer (**M-1**, **M-2**, **M-3**) was prepared through Knoevenagel condensation of 2-(2,6-dimethylpyran-4-ylidene)malononitrile (**7**) with monoaldehyde compound (**2**, **4**, **6**). The structures of monomer (**M-1**, **M-2**, **M-3**) were confirmed by <sup>1</sup>H NMR, <sup>13</sup>C NMR, and elemental analysis. In <sup>1</sup>H NMR spectroscopy of monomer (**M-2**), the coupling constant ( $J \sim 15.5$  Hz) of olefinic protons indicates that the Knoevenagel reaction afforded the pure all-trans isomers, which is further confirmed by the characterization of vibration band of trans double bond at 960 cm<sup>-1</sup> in the FT-IR spectra. The 2,7-Bis(4,4,5,5-tetramethyl-1,3,2-dioxaborolan-2-yl)-9,9-dihexylfluorene (**8**) was prepared according to previously reported methods. The polymerization reaction was proceeded by the well-known palladium-catalyzed Suzuki coupling reaction between bis(4,4,5,5-tetra methyl-1,3,2-dioxaborolane) fluorene (**8**) and varied functionalized dibromo aromatic monomer (**M-1**, **M-2**, **M-3**) [26]. The synthetic routes of copolymers are shown in Scheme 2. The <sup>1</sup>H NMR spectra of all the copolymers and their assignments shown in Fig. 1 are consistent with the proposed structure. NMR spectra clearly indicate that well defined the copolymers has been obtained.

All the copolymers exhibited excellent solubility in common organic solvents such as chloroform, tetrahydrofuran, dichloromethane, and chlorobenzene. Molecular weights and polydispersities of the resulting copolymers were determined by GPC analysis with the number average molecular weight ( $M_n$ ) of 5240–43,800 g/mol and PDI (polydispersity index,  $M_w/M_n$ ) of 1.49–4.2. Table 1 summarized the polymerization results including molecular weights, PDI and thermal stability of the copolymers. The steric hindrance of alkoxy and low solubility of the monomer **M-1** and **M-**



Scheme 1. Synthetic routes of the monomers.



**Scheme 2.** Synthetic routes of the copolymers.

**3**, which prevented the polymerization due to its low solubility, should be the main reason for the low polymerization of PFBMB and PFPMP. The large polydispersity in the molecular weight of PFTMT may be a result of the precipitation of copolymer from the reaction solution.

### 3.2. Thermal properties

All the copolymers exhibited good thermal stability with 5% weight-loss temperatures ( $T_d$ ) higher than 301 °C under  $\text{N}_2$  and high glass transition temperatures ( $T_g$ ) of 115–175 °C, as revealed by thermogravimetric analysis (TGA) and the differential scanning calorimetry (DSC), respectively (see Fig. 2). The high thermal stability of the resulting copolymers prevents the deformation of

the copolymer morphology and the degradation of active layer applied in PVCs.

### 3.3. Optical properties

The normalized UV–vis absorption spectra of PFBMB, PFTMT and PFPMP in dilute chloroform solution (concentration  $10^{-5}$  M) are shown in Fig. 3, and the main optical properties are listed in Table 2. PFBMB with the weak electron-donating dialkylfluorene moiety showed two absorption bands at 348 nm and 460 nm in dilute solution (Fig. 3a), which can be assigned to  $\pi$ - $\pi^*$  transition of the conjugated copolymer backbone and ICT interaction between the fluorene donor and BVM-based acceptor. Similarly, the absorption spectra of other copolymers (PFTMT and PFPMP) in dilute solutions

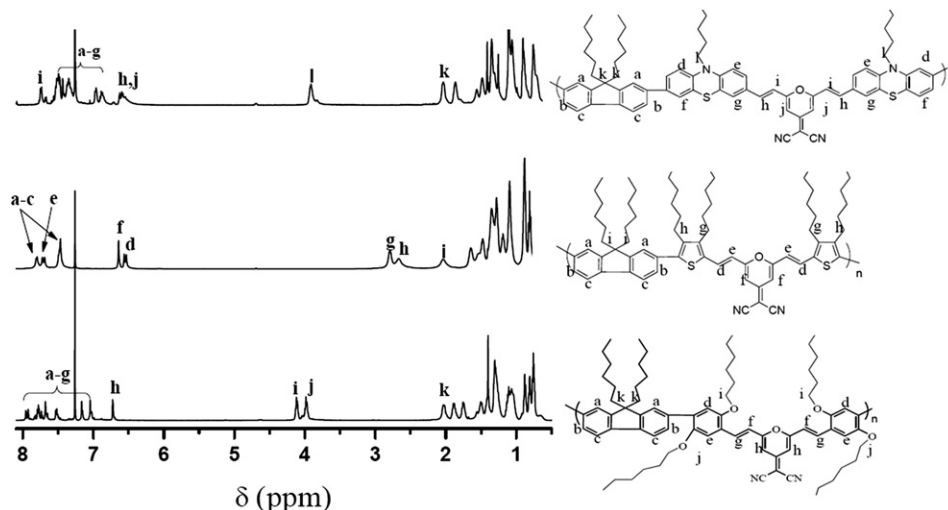


**Fig. 1.**  $^1\text{H}$  NMR spectra and chemical structures of PFBMB, PFTMT and PFPMP in  $\text{CDCl}_3$  solution.

**Table 1**  
Polymerization Results for Copolymers PFBMB, PFTMT and PFPMP.

Copolymer	$M_n$ (Kg/mol) <sup>a</sup>	$M_w$ (Kg/mol) <sup>a</sup>	PDI	$T_g^b$ (°C)	$T_d^c$ (°C)
PFBMB	5.24	8.28	1.58	116	353
PFTMT	43.8	183.8	4.20	115	380
PFPMP	6.16	9.20	1.49	175	301

<sup>a</sup> Calculated from GPC (eluent : THF; polystyrene standards).

<sup>b</sup> Determined by DSC at a heating rate of 20 °C/min under nitrogen.

<sup>c</sup> Temperature at 5% weight loss by a heating rate of 10 °C/min under nitrogen.

also showed two bands near 334, 335 nm and 482, 500 nm due to the  $\pi$ - $\pi^*$  transition and the ICT interaction, respectively. The solution absorption spectrum of PFPMP, with an absorption maximum ( $\lambda_{\max}^{\text{abs}}$ ) at 500 nm, is red-shifted compared to those of PFBMB ( $\lambda_{\max}^{\text{abs}} = 460$  nm), and PFTMT ( $\lambda_{\max}^{\text{abs}} = 482$  nm), which can be explained by much stronger ICT effect in PFPMP than that in PFBMB and PFTMT. Among these three copolymers, there is an alternating “D\*-(D-A-D)” structure, where the D\* is the donor of fluorene, and A is the PM-based acceptor unit which is bridged by varied electron-donating ability donor D (1,4-linked styryl; 2,5-linked thiophenevinyl; 1,4-linked phenothiazinevinyl). If the bridged-D possesses the strong electron-donating ability, the electronic delocalization degree and the ICT intensity of the copolymer will be enhanced. Since the order of the electron-donating abilities of the three bridged-D is benzene < thiophene < phenothiazine, the strongest electron-donating ability of phenothiazine compared to benzene and thiophene improves the effective conjugation length along copolymer backbone, resulting in an increase in the ICT strength and thus electronic delocalization [27]. Moreover, the relatively high absorption coefficients ( $\epsilon_{\max}$ ) could be calculated from Beer's law equation with the same dilute concentration of the copolymers in chloroform, which assures the copolymers can absorb enough photons.

Fig. 3b shows the optical absorption spectra of thin films of the copolymers. The thin film absorption spectra are generally similar in shape to those in dilute solution. The maximum absorption peak of PFBMB at visible region shows a 7 nm red shift between in solutions and thin films. In the case of PFTMT and PFPMP, the absorption spectra in thin films also exhibit 9 nm and 12 nm red shift, respectively, which can be explained by the formation of  $\pi$ - $\pi$  stacking structure in the solid state that could facilitate charge transportation for photovoltaic applications. The small red shift between in solutions and thin films of the three copolymers maybe caused by the nonplanar conformations due to the fluorene and

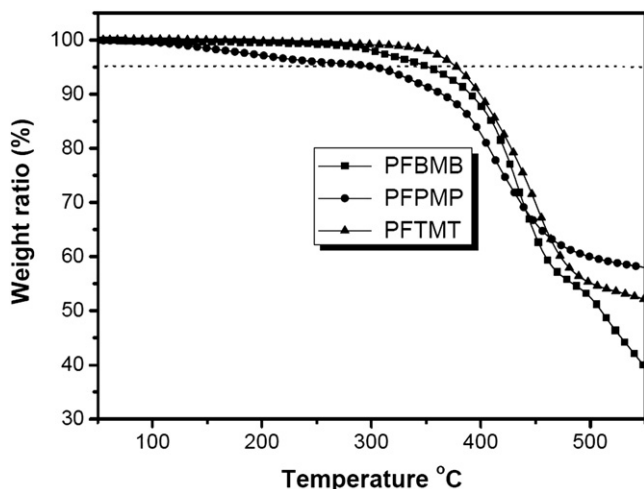


**Fig. 2.** TGA thermograms of the copolymers.

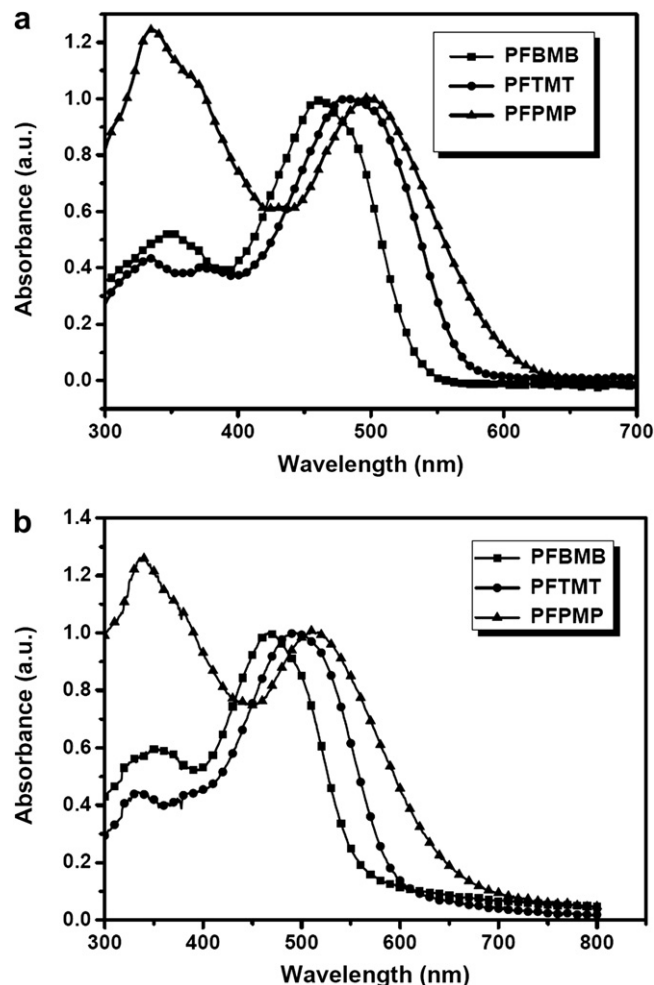


**Fig. 3.** Normalized absorption spectra of the copolymers (a) in chloroform solutions with the concentration of  $10^{-5}$  mol/L; (b) films spin-coated from a 10 mg/mL chloroform solution.

phenothiazine moieties and the long alkyl side chains can induce the twist of the copolymer backbone, which is not beneficial to the  $\pi$ - $\pi$  stacking in the solid state [29].

The ICT absorption bands of the three copolymers are tuned from 467 to 512 nm, and the optical band gap  $E_{g,\text{opt}}$  of the copolymers derived from the absorption edge of the thin film spectra is in the range of 2.23–1.92 eV (Table 2). As expected, among the three copolymers, PFPMP with the strongest intramolecular charge transfer interaction thus has the lowest optical band gap of 1.92 eV, which is lower than that of poly(3-alkylthiophene) homopolymer ( $\sim 2.0$  eV) [28,30]. It is evident that the ICT interaction between bridged-D and acceptor moieties in D\*-(D-A-D) copolymers is a practical approach to lower the band gap. We also investigated the photoluminescence properties of the synthesized copolymers in solutions and films. It has to be noted that all the copolymers discussed here are poorly emissive except PFTMT in solution. The observed strong quenching of the luminescence is in good agreement with the occurrence of an ICT process [31].

To further understand the optical properties of PFBMB, PFTMT and PFPMP, we have carried out the molecular orbital distribution calculations of the basic structure units (D\*-(D-A-D) model) of the three copolymers using quantum mechanical package Gaussian 03. The optimum geometry and electron-state-density distribution of the highest occupied molecular orbital (HOMO) and the lowest unoccupied molecular orbital (LUMO) were calculated by using the

**Table 2**  
Optical and electrochemical data of the PFBMB, PFTMT and PFPMP.

Copolymer	In solution <sup>a</sup>			In film <sup>b</sup>		$E_{\text{Ox}}^{\text{onset}}$	$E_{\text{Red}}^{\text{onset}}$	Electrochem. $E_{g,ec}$ (eV)	Optical <sup>c</sup> $E_{g,opt}$ (eV) <sup>c</sup>
	$\lambda_{\text{max}}^{\text{abs}}$ [nm]	$\epsilon_{\text{max}}$ ([M <sup>-1</sup> cm <sup>-1</sup> ])	$\lambda_{\text{edge}}$ [nm]	$\lambda_{\text{max}}^{\text{abs}}$ [nm]	$\lambda_{\text{edge}}$ [nm]	(V)/HOMO(eV)	(V)/LUMO(eV)		
PFBMB	460 (60230)		532	467	556	0.94/−5.64	−1.39/−3.31	2.38	2.23
PFTMT	483 (49270)		568	492	581	0.91/−5.61	−1.32/−3.38	2.23	2.13
PFPMP	500 (70369)		604	512	646	0.47/−5.17	−1.35/−3.35	1.78	1.92

<sup>a</sup>  $1 \times 10^{-5}$  M in anhydrous chloroform.

<sup>b</sup> Spin-coated from a 10 mg/mL chloroform solution.

<sup>c</sup> The optical band gap ( $E_{g,opt}$ ) was obtained from absorption edge.

density functional theory (DFT) as approximated by the B3LYP functional and employing the 6-31G\* basis set (see in Fig. 4). Abinitio calculations on the model compound for the three copolymers show that the different degree of torsion between D\* and D lead to the nonplanar molecule, which weakens the electrons to be delocalized within the molecule by conjugation, and also decreased the  $\pi$ - $\pi$  stacking structure in the solid state. This result is in agreement with the slight red shift of copolymers between in solutions and thin films. The HOMO state density was distributed some extent over  $\pi$ -conjugated molecule, the electron density of LUMO was mainly localized on the PM moiety with some extending to bridged-D, which suggests that the transition is accompanied by ICT from D\* and D units to the PM moiety, and as a result, the low band gap of the copolymers are due to the introduction of the PM segment.

### 3.4. Electrochemical properties

Fig. 5 shows the cyclic voltammetry (CV) diagrams of the copolymers using TBAPF<sub>6</sub> as supporting electrolyte in acetonitrile solution with platinum button working electrodes, a platinum wire counter electrode and an Ag/AgNO<sub>3</sub> reference electrode under the N<sub>2</sub> atmosphere. Ferrocene was used as the internal standard. The

onset oxidation potentials ( $E_{\text{Ox}}^{\text{onset}}$ ) of the three copolymers are observed in the range of 0.47–0.94 V. The onset reduction potentials ( $E_{\text{Red}}^{\text{onset}}$ ) are almost the same for the three copolymers (−1.35 V). The redox potential of Fc/Fc<sup>+</sup> which has an absolute energy level of −4.8 eV relative to the vacuum level for calibration is located at 0.1 V in 0.1 M TBAPF<sub>6</sub>/acetonitrile solution [32]. So the evaluation of HOMO and LUMO levels as well as the band gap ( $E_{g,ec}$ ) could be done according to the following equations:

$$\text{HOMO(eV)} = -e(E_{\text{Ox}}^{\text{onset}} + 4.7)(\text{eV})$$

$$\text{LUMO(eV)} = -e(E_{\text{Red}}^{\text{onset}} + 4.7)(\text{eV})$$

$$E_{g,ec} = E_{\text{Ox}}^{\text{onset}} - E_{\text{Red}}^{\text{onset}} (\text{eV})$$

where  $E_{\text{Ox}}^{\text{onset}}$  and  $E_{\text{Red}}^{\text{onset}}$  are the measured potentials relative to Ag/Ag<sup>+</sup>. The electrochemical properties as well as the energy level parameters of copolymers are listed in Table 2.

The estimated HOMO and LUMO energy levels of PFBMB are −5.64 and −3.31 eV, respectively. The LUMO energy levels of PFTMT and PFPMP are −3.38 and −3.35 eV, which are very similar to that of PFBMB. Therefore, the substitution of bridged-D with varied electron-donating ability moieties has slight effect on the

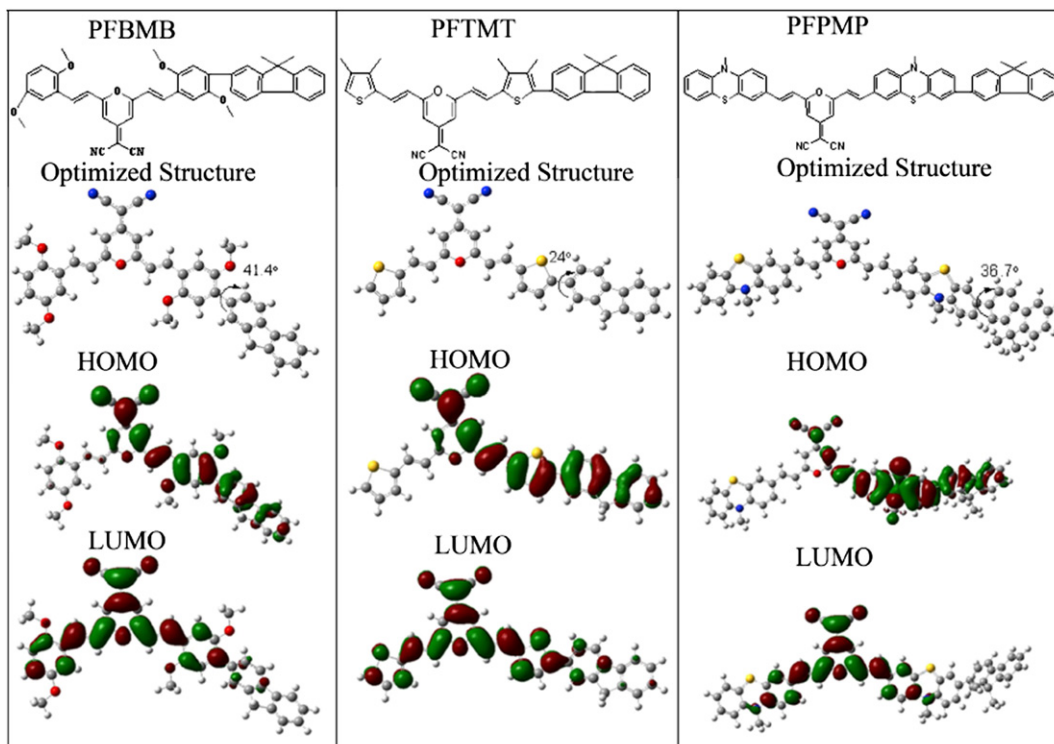


**Fig. 4.** Molecular orbital surfaces of the HOMO and LUMO of D\*–D–A–D model obtained at B3LYP/6-31G\* level.

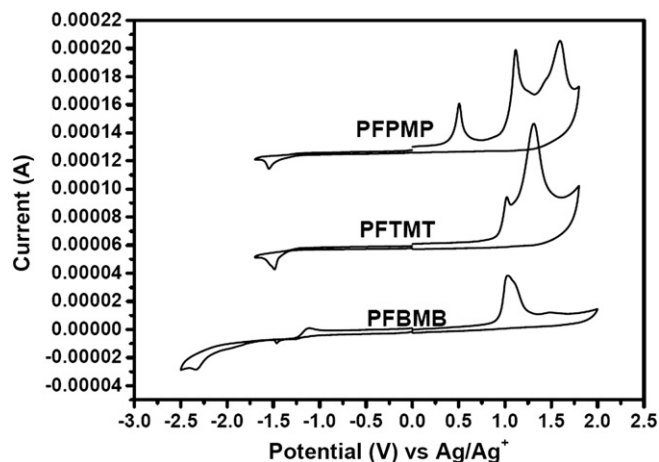


Fig. 5. Cyclic voltammetry curves of PFBMB, PFTMT, PFPMP films on platinum electrode in 0.1 mol/L *n*-Bu<sub>4</sub>NPF<sub>6</sub> in CH<sub>3</sub>CN solution, at a scan rate of 100 mV/s.

reduction potential of the copolymers, which is consistent with molecular orbital distribution calculations that the electron density of LUMO was mainly localized on the PM moiety with some extending to bridged-D. Besides, the relatively low LUMO energy levels of the three copolymers result from the stronger reduction of PM-based acceptor unit. On the other hand, the HOMO energy levels of copolymers behave quite differently. The HOMO energy levels of the copolymers PFBMB, PFTMT and PFPMP are in the range of  $-5.64$  to  $-5.17$  eV, which are clearly affected by the varied electron-donating ability of the three bridged-D due to the modulation of the ICT strength. The HOMO levels of PFBMB ( $-5.64$  eV), PFTMT ( $-5.61$  eV) and PFPMP ( $-5.17$  eV) are gradually increased with the enhanced electron-donating ability of the three bridged-D. Generally, the stronger electron-donating ability of bridged-D resulted in a higher HOMO energy level.

The HOMO energy level of the donor copolymers is very important for high performance photovoltaic cell. Firstly, the copolymers should have good air stability with HOMO energy level being below the air oxidation threshold (ca.  $-5.2$  eV) [33,39]. Secondly, the relatively low HOMO level of the copolymers can allow a high open circuit potential ( $V_{oc}$ ) value for the photovoltaic cell [22]. A complete picture of the band structure of the copolymers is presented in Fig. 6. The first dashed line indicates the threshold for air stability, and the second dashed line represents the threshold value for an effective charge transfer from the copolymers to PCBM ( $-4.3$  eV) [39]. Both the HOMO energy levels and LUMO energy levels of the copolymers are close to the ideal range. The destabilization of HOMO and stabilization of LUMO level result in reduced band gaps, which also demonstrated the significance of intramolecular charge transfer through the D–A structures inside the copolymers. Although there is deviation between the optical band gap ( $E_{g,opt}$ ) and electrochemical band gap ( $E_{g,ec}$ ), the trend between the band gap and copolymer structure is similar. So, the HOMO energy level and band gap of the copolymers can be controlled strictly by introducing different electron-donating ability electron donors.

### 3.5. Photovoltaic properties

In order to investigate the photovoltaic properties of the copolymers, the BHJ photovoltaic cells with a structure of ITO/PEDOT-PSS/copolymers:PCBM/LiF/Al were fabricated, where the copolymers were used as donors and PCBM as the acceptor [34]. The weight ratios of blend films (copolymers:PCBM) were

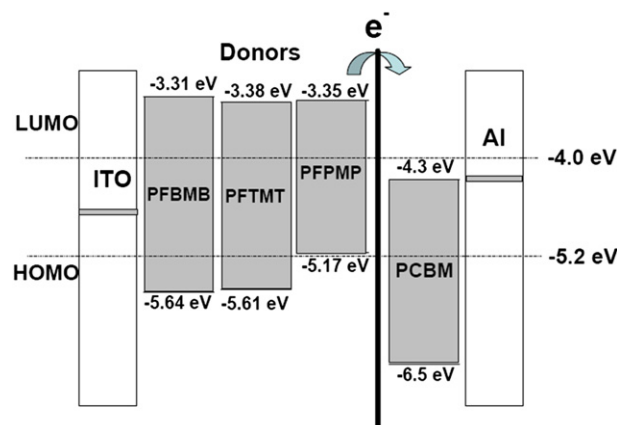


Fig. 6. Band diagram for accepting PCBM and donor PFBMB, PFTMT, and PFPMP copolymers. Dashed lines indicate the thresholds for air stability (5.2 eV) and effective charge transfer PCBM (4.3 eV).

investigated from 1:1 to 1:4. It is known that solvents used for the preparation of the active layer have a strong impact on the performance of the cell [35]. Here, we chose chlorobenzene for the three copolymers in order to obtain the films with the relative good quality. The devices were characterized in the dark and under solar simulator AM1.5 ( $100 \text{ mW/cm}^2$ ) with simultaneous recording of their current–voltage characteristics. The current–voltage characteristics of the photovoltaic cell based on PFBMB:PCBM, PFTMT:PCBM and PFPMP:PCBM with weight ratio (1:3 w/w) showed the best performance, which are presented in Fig. 7. The photovoltaic parameters of the photovoltaic cells are summarized in Table 3.

The cells based on PFBMB:PCBM (1:3 w/w) and PFTMT:PCBM (1:3 w/w) showed an open circuit voltage ( $V_{oc}$ ) of 0.78 V and 0.80 V, a short circuit current ( $J_{sc}$ ) of  $0.11 \text{ mA/cm}^2$  and  $0.20 \text{ mA/cm}^2$ , a fill factor (FF) of 0.27 and 0.28, giving a power conversion efficiency (PCE) of 0.02% and 0.04%, respectively. The low  $J_{sc}$  of the cells may be caused by the weak ICT interaction inside PFBMB and PFTMT and the bad aggregated configuration in solid state of PFTMT:PCBM blend film which leads to the low absorption of solar spectrum and hindered charge transport. However, greatly enhanced device performance was obtained for the other two cells based on

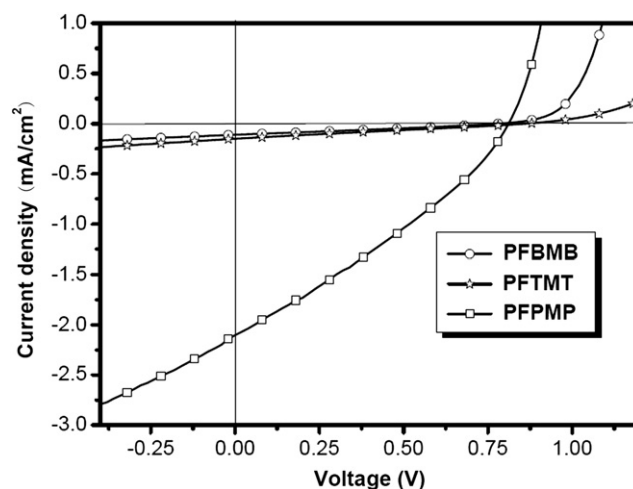


Fig. 7. Current–voltage characteristics of copolymer photovoltaic cells based on PFBMB, PFTMT and PFPMP in the dark and under illumination of AM 1.5,  $100 \text{ mW/cm}^2$  white light.

**Table 3**

Characteristic current–voltage parameters from device testing at standard AM 1.5G conditions and blend films roughness of AFM measurement.

	Copolymer/PCBM (w/w ratio)	$V_{oc}$ (V) <sup>a</sup>	$J_{sc}$ (mA/cm <sup>2</sup> ) <sup>a</sup>	FF <sup>a</sup>	RMS (nm) <sup>b</sup>	PCE (%) <sup>a</sup>
PFBMB	1:3	0.78	0.11	0.27	60.89	0.02
PFTMT	1:3	0.80	0.20	0.28	5.73	0.04
PFPMMP	1:3	0.82	2.1	0.30	1.79	0.52

<sup>a</sup> Photovoltaic properties of copolymer/PCBM-based devices spin-coated from a chlorobenzene solution for PFBMB (1:3 w/w), PFTMT (1:3 w/w) and PFPMMP (1:3 w/w).

<sup>b</sup> Root mean-square (RMS) roughness from AFM measurement.

PFPMMP:PCBM (1:3 w/w) with  $V_{oc}$  of 0.82,  $J_{sc}$  of 2.1 mA/cm<sup>2</sup>, FF of 0.30, and PCE of 0.52%, respectively. The reason for the improvement PCE could be explained by the strong ICT interaction and better  $\pi$ – $\pi$  stacking of PFPMMP in the solid state.

To gain better insight into what might be controlling the low short circuit current and open circuit voltage, atomic force microscopy (AFM) was used to examine the surface topography of the films. Film morphology of the active layer, i.e. the blend film of the donor copolymer and the acceptor (e.g. PCBM) has been found to be one of the key elements in determining the PCE of copolymer photovoltaic cell [36]. Fig. 8a–c shows the AFM height images of PFBMB:PCBM, PFTMT:PCBM, PFPMMP:PCBM blend films with the same weight ratio (1:3 w/w) for effective comparison and further elucidation of the difference in PV performance. As is clearly evidenced by AFM, the PFBMB:PCBM blend film shows a high coarse surface with the root mean square (RMS) of 60.89 nm (Fig. 8a and Table 3), and substantial PCBM grain-aggregation with the size distribution around 1.50  $\mu$ m are almost homogeneously dispersed in the PFBMB matrix, which results in a most large-scale phase separation, decreased diffusional escape probability for mobile charge carriers and hence increased recombination. This is fully consistent with the low short circuit obtained for the PFBMB:PCBM cell (0.11 mA/cm<sup>2</sup>). Compared with the PFBMB:PCBM blend film, the blend film of PCBM and PFTMT with a relatively strong electron-donating abilities moiety, thiophene instead of benzene, shows a lower degree of grain-aggregation with the size distribution around 150 nm, the relative flat surface with the RMS of 5.73 nm (Fig. 8b) and smaller phase separation, which lead to an improvement of the short circuit current for the PFTMT:PCBM cell (0.20 mA/cm<sup>2</sup>). In the case of PFPMMP:PCBM blend film (Fig. 8c), an even stronger electron-donating abilities moiety phenothiazine was brought in, and

a high degree of homogeneity is observed for the film. Since PFPMMP and PCBM molecules have good miscibility, increased interfacial area is expected, and the  $J_{sc}$  of PFPMMP:PCBM (1:3 w/w) based device increases to 2.1 mA/cm<sup>2</sup>, which is more than 13 times higher than that of PFTMT:PCBM based device. It has been recently reported that chemical similarity between the functional groups attached to the donor copolymers and the fullerene can effectively affect the formation of films with uniform and stable nanophase morphologies [37]. In the present case, the significant morphological difference between the three blend copolymer films suggests that similar chemical polarity of the D–A copolymers with PCBM by adjusting the ICT intensity may improve the miscibility between them in the blend film, thereby efficiently suppressing the tendency of the PCBM molecules to phase segregate into microscale clusters or uniform morphologies.

Fig. 9 depicts photocurrent action spectra for the PFBMB:PCBM (1:3 w/w), PFTMT:PCBM (1:3 w/w), PFPMMP:PCBM (1:3 w/w) photovoltaic devices under monochromatic illumination. The external quantum efficiency or incident photon-to-current efficiency, IPCE (%), is displayed as a function of wavelength. Comparing the IPCE curves of PFBMB:PCBM, PFTMT:PCBM and PFPMMP:PCBM, it can be seen that the IPCE values of PFBMB:PCBM and PFTMT:PCBM in the wavelength ranging from 400 to 600 nm are similar and showed extremely low values (no more than 2%). However, the IPCE curve of PFPMMP:PCBM shows a significantly increased spectral response in the visible region. The maximum IPCE values of the device based on PFPMMP:PCBM is 20% at 489 nm in the wavelength ranging from 400 to 600 nm. It is further confirmed that the PFPMMP:PCBM based device with higher IPCE values obtained higher  $J_{sc}$ .

Furthermore, as discussed above, the  $V_{oc}$  is directly governed by the difference between the HOMO energy levels of the donor and the LUMO of the acceptor. However, several other parameters must be taken into account such as carrier recombination, resistance related to thickness of the active layer and degree of phase separation between the components in the blend, which can modify the energetically expected  $V_{oc}$  value. Therefore, although the HOMO energy levels of PFBMB and PFTMT are higher than that of PFPMMP, the  $V_{oc}$  value of PFBMB and PFTMT-based device was a bit lower than that of PFPMMP-based devices. The relative low  $V_{oc}$  for PFBMB and PFTMT-based device could be explained by the large numbers of carrier recombination due to the obvious grain-aggregation and large-scale blend phase separation. But all the three copolymers have a satisfying  $V_{oc}$  (around 0.80 V), which is higher than the P3HT:PCBM based device (0.6 V) [38].

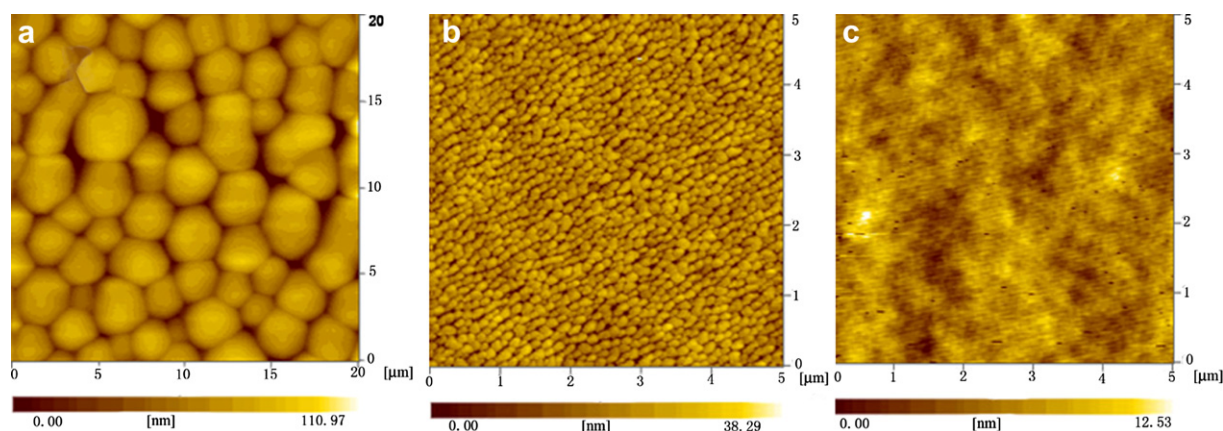


**Fig. 8.** Topography image obtained by tapping-mode AFM showing the morphology of the blend films spin-coated from chlorobenzene for (a) PFBMB/PCBM (w/w, 1:3) (size 20  $\mu$ m  $\times$  20  $\mu$ m); (b) PFTMT/PCBM (w/w, 1:3) (size 5  $\mu$ m  $\times$  5  $\mu$ m); (c) PFPMMP/PCBM (w/w, 1:3) (size 5  $\mu$ m  $\times$  5  $\mu$ m).

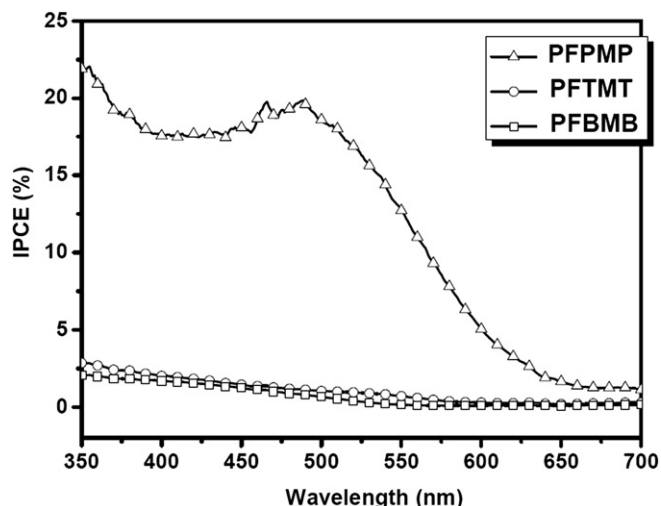


Fig. 9. The incident photon-to-current conversion efficiency (IPCE) spectra of devices fabricated with PFBMB/PCBM, PFTMT/PCBM and PFPMP/PCBM system.

#### 4. Conclusions

We have designed and synthesized three novel D–A conjugated copolymers consisting of PM as acceptor coupled to fluorene by different electron-donating ability bridged moieties. Optical property and molecular orbital distribution calculations investigations unequivocally indicate that these new copolymers exhibit enhanced ICT bands in solid state by with electron-donating ability increasing of the bridged-D, which lead to an extension of their absorption spectral range. The copolymers had optical band gaps in the range of 1.92–2.23 eV. The HOMO and LUMO energy levels of resulting copolymers can be fine-tuned as demonstrated from the investigation of electrochemical study. The relatively low HOMO energy levels promised good air stability and high  $V_{oc}$  for photovoltaic cells application. The miscibility between copolymers and PCBM can be adjusted by the ICT intensity. The better miscibility between copolymers and PCBM, the smaller scale phase separation and better uniform film will be formed. The highest PCE value of 0.52% was obtained from the device based on PFPMP with a strongest electron-donating ability bridged-D, which was more than 13 times higher than that of the device based on PFTMT (0.04%). Although the power conversion efficiencies for these unoptimized photovoltaic devices are still not sufficiently high, their tunable electronic properties provide an understanding on how the copolymer structures affect the device characteristics.

#### Acknowledgments

This work was supported by the State Key Development Program for Basic Research of China (Grant No.2009CB623605), the National Natural Science Foundation of China (Grant No.50673035, 20874035), Program for New Century Excellent Talents in Universities of China Ministry of Education, the 111 Project (Grant No. B06009), and the Project of Jilin Province (20080305), Yaowen Li

would like to thank the financial support of the Project 20091008 from Graduated Innovation Fund of Jilin University.

#### References

- (a) Yu G, Gao J, Hummelen JC, Wudl F, Heeger AJ. *Science* 1995;270:1789–91; (b) Gunes S, Neugebauer H, Sariciftci NS. *Chem Rev* 2007;107:1324–38.
- (a) Chen CP, Chan SH, Chao TC, Ting C, Ko BT. *J Am Chem Soc* 2008;130:12828–33; (b) Blouin N, Michaud A, Gendron D, Wakim S, Blair E, Plesu RN, et al. *J Am Chem Soc* 2008;130:732–42.
- Chang YT, Hsu SL, Chen GY, Su MH, Singh TA, Diau EWG, et al. *Adv Funct Mater* 2008;18:2356–65.
- (a) Liang YY, Wu Y, Feng DQ, Tsai ST, Son HJ, Li G, et al. *J Am Chem Soc* 2009;131:56–7; (b) Zhang SM, He C, Liu Y, Zhan XW, Chen JW. *Polymer* 2009;50:3595–9.
- Sariciftci NS, Smilowitz L, Heeger AJ, Wudl F. *Science* 1992;258:1474–6.
- Ma WL, Yang CY, Gong X, Lee KH, Heeger AJ. *Adv Funct Mater* 2005;15:1617–22.
- Coakley KM, McGehee MD. *Chem Mater* 2004;16:4533–42.
- (a) van Müllekom HAM, Vekemans JAJM, Havinga EE, Meijer EW. *Mater Sci Eng R* 2001;32:1–40; (b) Tsai FC, Chang CC, Liu CL, Chen WC, Jenekhe SA. *Macromolecules* 2005;38:1958–66.
- (a) Neef CJ, Brotherton ID, Ferraris JP. *Chem Mater* 1999;11:1957–8; (b) Lee K, Sotzing GA. *Macromolecules* 2001;34:5746–7; (c) Campos LM, Tontcheva A, Gunes S, Sonmez G, Neugebauer H, Sariciftci NS, et al. *Chem Mater* 2005;17:4031–3.
- Zhang ZG, Zhang KL, Liu G, Zhu CX, Neoh KG, Kang ET. *Macromolecules* 2009;42:3104–11.
- (a) Zhang FL, Mammo W, Andersson LM, Admassie S, Andersson MR, Inganäs L, et al. *Adv Mater* 2006;18:2169–73; (b) Wong WY, Wang XZ, He Z, Djuricic AB, Yip CT, Cheung KY, et al. *Nat Mater* 2007;6:521–7.
- Halls JMM, Pichler K, Friend RH, Moratti SC, Holmes AB. *Appl Phys Lett* 1996;68:3120–2.
- Svensson M, Zhang FL, Veenstra SC, Verhees WJH, Hummelen JC, Kroon JM, et al. *Adv Mater* 2003;15:988–91.
- Boudreaux PT, Michaud A, Leclerc M. *Macromol Rapid Commun* 2007;28:2176.
- Blouin N, Michaud A, Leclerc M. *Adv Mater* 2007;19:2295–300.
- Liao L, Dai LM, Smith A, Durstock M, Lu JP, Ding JF, et al. *Macromolecules* 2007;40:9406–12.
- Moullé AJ, Tsami A, Bünnagel TW, Forster M, Kronenberg NM, Scharber M, et al. *Chem Mater* 2008;20:4045–50.
- Agrawal AK, Jenekhe SA. *Chem Mater* 1996;8:579–89.
- Cui Y, Zhang X, Jenekhe SA. *Macromolecules* 1999;32:3824–6.
- Yasuda T, Sakai Y, Aramaki S, Yamamoto T. *Chem Mater* 2005;17:6060–8.
- Lee SK, Jung BJ, Ahn T, Jung YK, Lee JI, Kang IN, et al. *J Polym Sci A Polym Chem* 2007;45:3380–90.
- Li YW, Xue LL, Li H, Li ZF, Xu B, Wen SP. *Macromolecules* 2009;42:4491–9.
- Maruyama S, Kawanishi Y. *J Mater Chem* 2002;12:2245–9.
- Alam MM, Jenekhe SA. *Chem Mater* 2002;14:4775–80.
- Woods LL. *J Am Chem Soc* 1958;80:1440–2.
- Burn PL, Holmes AB, Kraft A, Bradley DDC, Brown AR, Friend RH, et al. *Nature* 1992;356:47–9.
- Wu PT, Kim FS, Champion RD, Jenekhe SA. *Macromolecules* 2008;41:7021–8.
- Chen TA, Wu X, Rieke RD. *J Am Chem Soc* 1995;117:233–44.
- Li YW, Xue LL, Xia HJ, Xu B, Wen SP, Tian WJ. *J Polym Sci A Polym Chem* 2008;46:3970–84.
- Babel A, Jenekhe SA. *J Phys Chem B* 2003;107:1749–54.
- Sophie R, Antonio C, Philippe L, Olivier A, Pierre F, Jean R. *J Am Chem Soc* 2006;128:3459–66.
- Pommerehne J, Vestweber H, Guss W, Mahrt RF, Bassler H, Porsch M, et al. *Adv Mater* 1995;7:551–4.
- Leeuw DMD, Simenon MMJ, Brown AR, Einerhand REF. *Synth Met* 1997;87:53–9.
- Li G, Shrotriya V, Huang J, Yao Y, Moriarty T, Emery K, et al. *Nat Mater* 2005;4:864–8.
- Shaheen SE, Brabec CJ, Sariciftci NS. *Appl Phys Lett* 2001;78:841–3.
- (a) Yang F, Shtein M, Forrest SRJ. *Appl Phys Lett* 2005;98:014906/1–10; (b) Hoppe H, Sariciftci NS. *J Mater Chem* 2006;16:45–61.
- Zhou ZY, Chen XW, Holdcroft S. *J Am Chem Soc* 2008;130:11711–8.
- Woo CH, Thompson BC, Kim BJ, Toney MF, Fréchet JM. *J Am Chem Soc* 2008;130:16324–9.
- Thompson BC, Kim YG, Reynolds JR. *Macromolecules* 2005;38:5359–62.